Supplementary Information for

Gas Evolution in Ruddlesden-Popper-type Intercalation Cathodes in All-Solid-State Fluoride-Ion-Batteries: Implications on Battery Performance and Synthesis of Highly Oxidized Oxyfluorides

Tommi Hendrik Aalto[a], Jonas Jacobs[b], Felix Frey[a], Dörthe Schiewe[c], Oliver Clemens[a,*]

[a] University of Stuttgart, Institute for Materials Science, Department of Chemical Materials Synthesis, Heisenbergstraße 3, 70569 Stuttgart, Germany

[b] Martin Luther University Halle-Wittenberg, Department of Chemistry, Inorganic Chemistry, Kurt-Mothes-Straße 2, 06120 Halle, Germany

[c] University of Stuttgart, Institute for Chemical Process Engineering, Böblinger Straße 78, 70199 Stuttgart, Germany

* Corresponding Author:

Prof. Dr. Oliver Clemens

Email: oliver.clemens@imw.uni-stuttgart.de

Fax: +49 711 685 51933

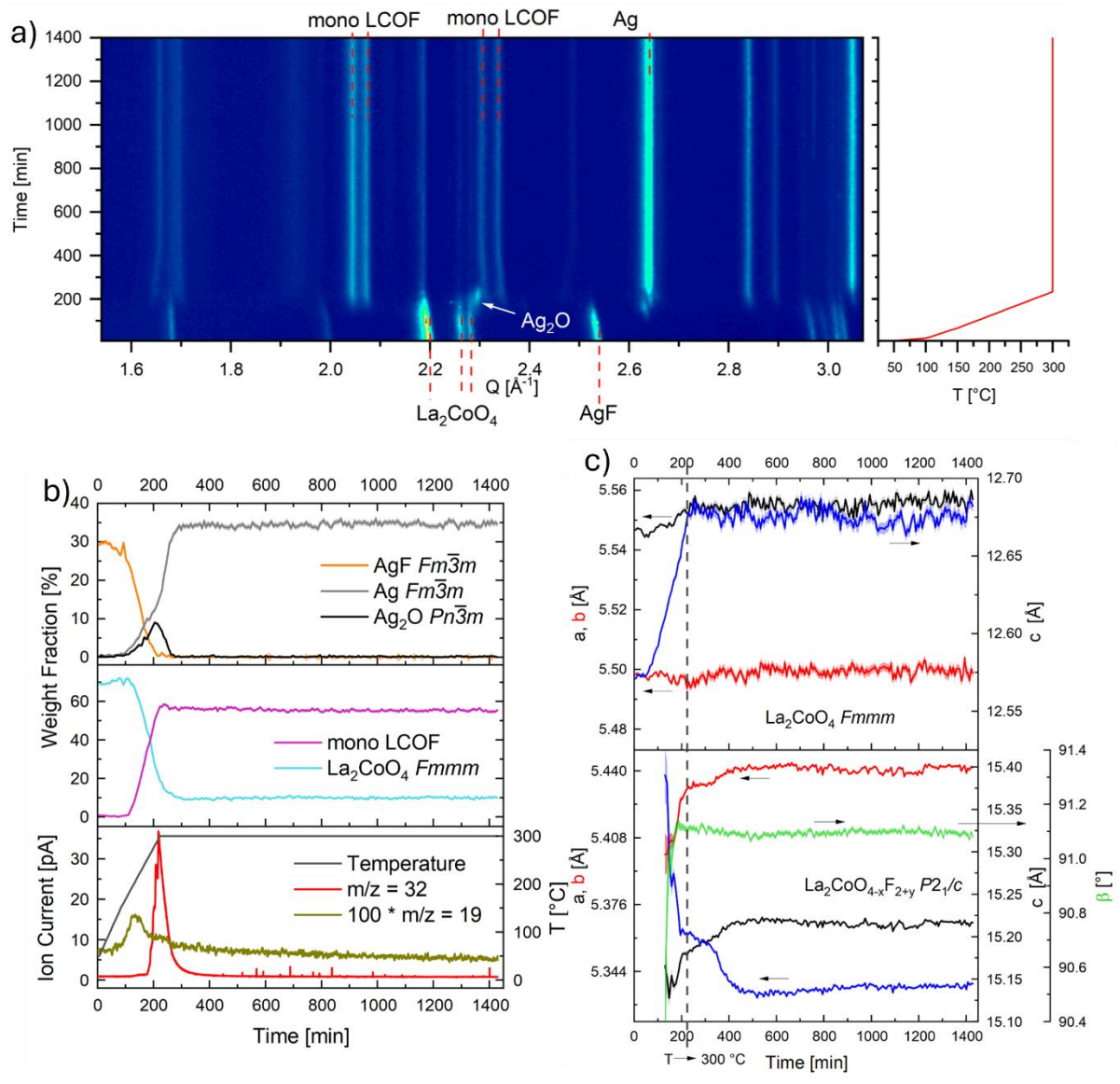

Figure S 1: a) Heatmap-Plot of the VTXRD patterns of La_2CoO_4 obtained during fluorination using three molar equivalents of AgF. (b) Weight fractions obtained by Rietveld refinement of AgF, Ag_2O, Ag; La_2CoO_4 Fmmm and mono LCOF as well as the ion current for m/z = 32 and m/z = 19 along with the temperature in the in situ XRD MS fluorination. (c) lattice parameters of both RP-type phases during the fluorination reaction.

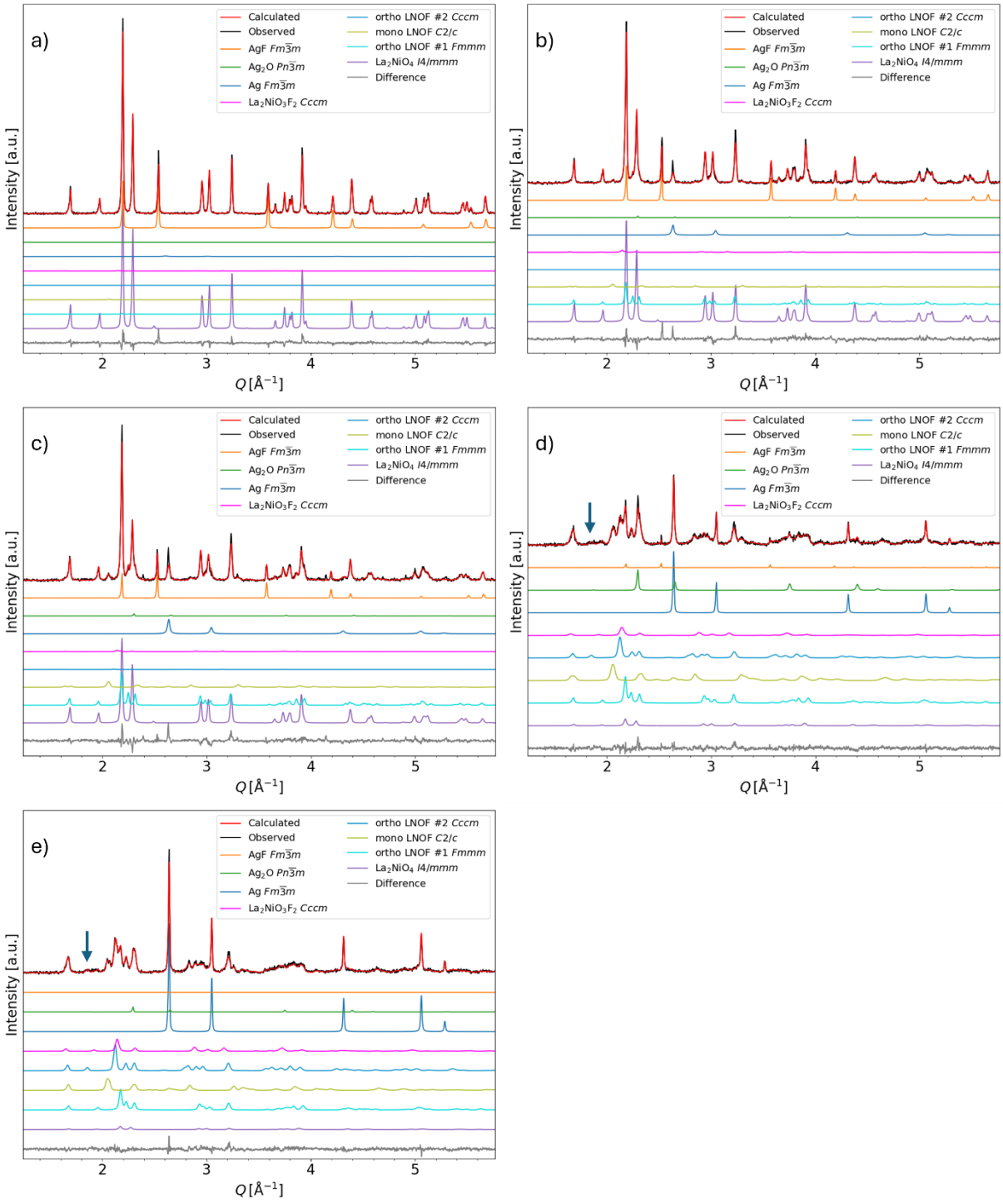

Figure S 2: Plots of selected scans and Rietveld-refinements of the XRD-MS measurement of the La_2NiO_4 - AgF reaction at (a) 6 minutes (b) 148 minutes (c) 167 minutes (d) 250 minutes (e) 319 minutes. The dark blue arrow marks the small indicator reflection for ortho LNOF #2.

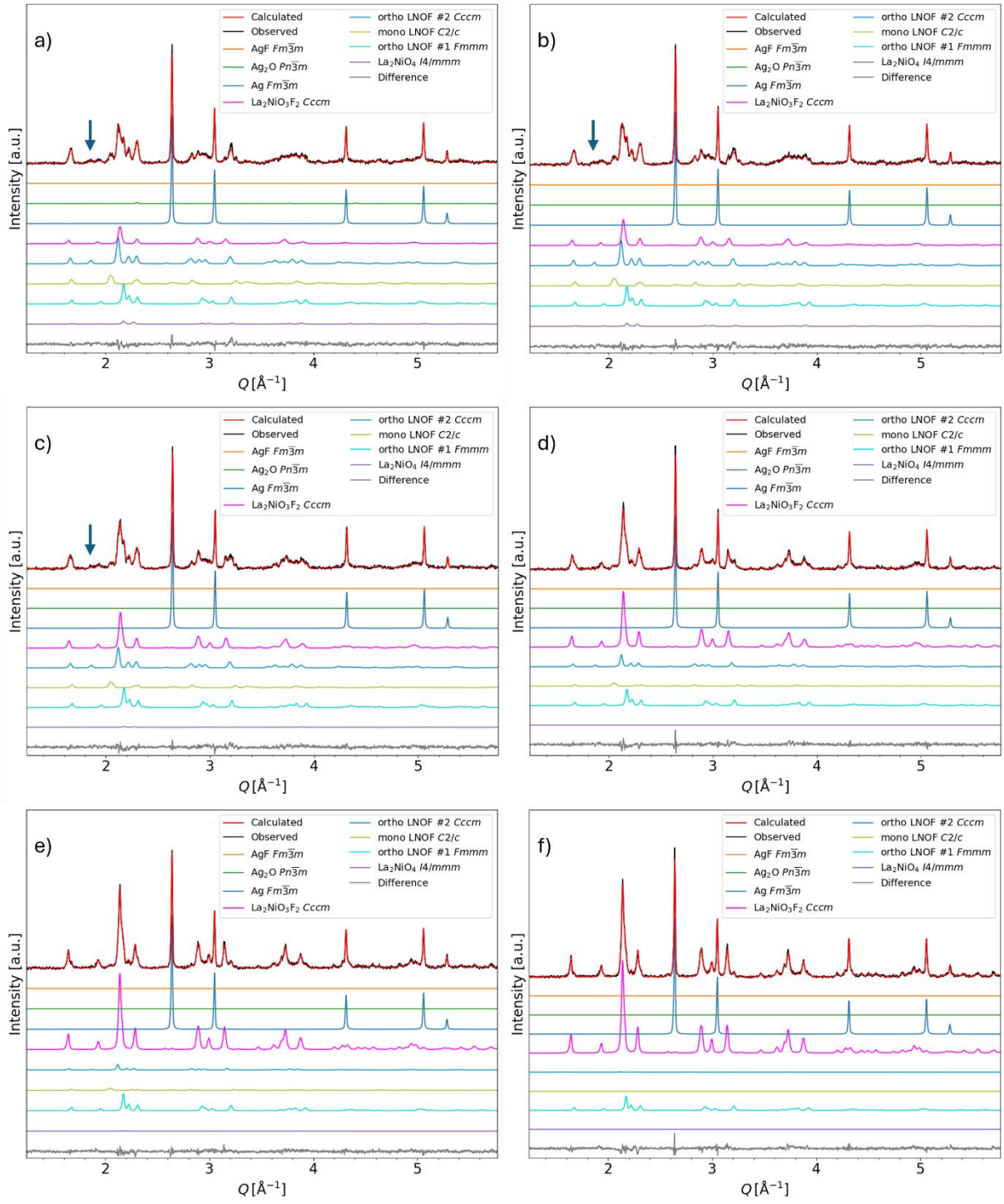

Figure S 3: plots of selected scans and Rietveld-refinements of the XRD-MS measurement of the La_2NiO_4 - AgF reaction at (a) 388 minutes (b) 456 minutes (c) 525 minutes (d) 732 minutes (e) 1076 minutes and (f) 1503 minutes. The dark blue arrow marks the small indicator reflection for ortho LNOF #2.

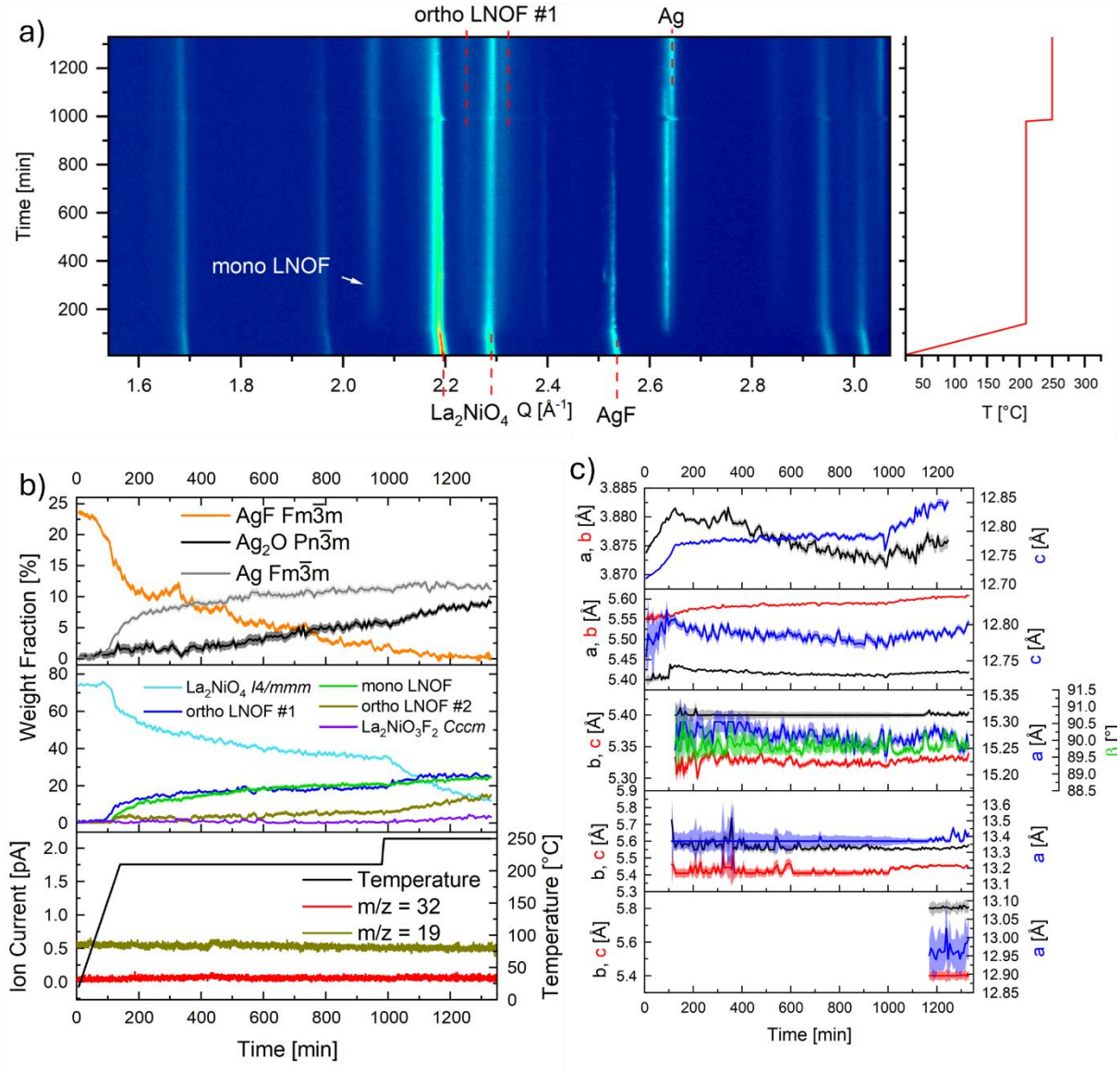

Figure S 4: (a) Heatmap-Plot of the VTXRD patterns of La_2NiO_4 obtained during fluorination using two molar equivalents of AgF with constant-temperature segments at 210 °C and 250 °C. (b) Weight fractions obtained by Rietveld refinement of AgF, Ag_2O, Ag; La_2NiO_4 I4/mmm, ortho LNOF #1, mono LNOF, ortho LNOF #2 and $La_2NiO_3F_2$ Cccm as well as the ion current for m/z = 32 and m/z = 19 along with the temperature in the in situ XRD MS fluorination. (c) lattice parameters of all RP-type phases during the fluorination reaction

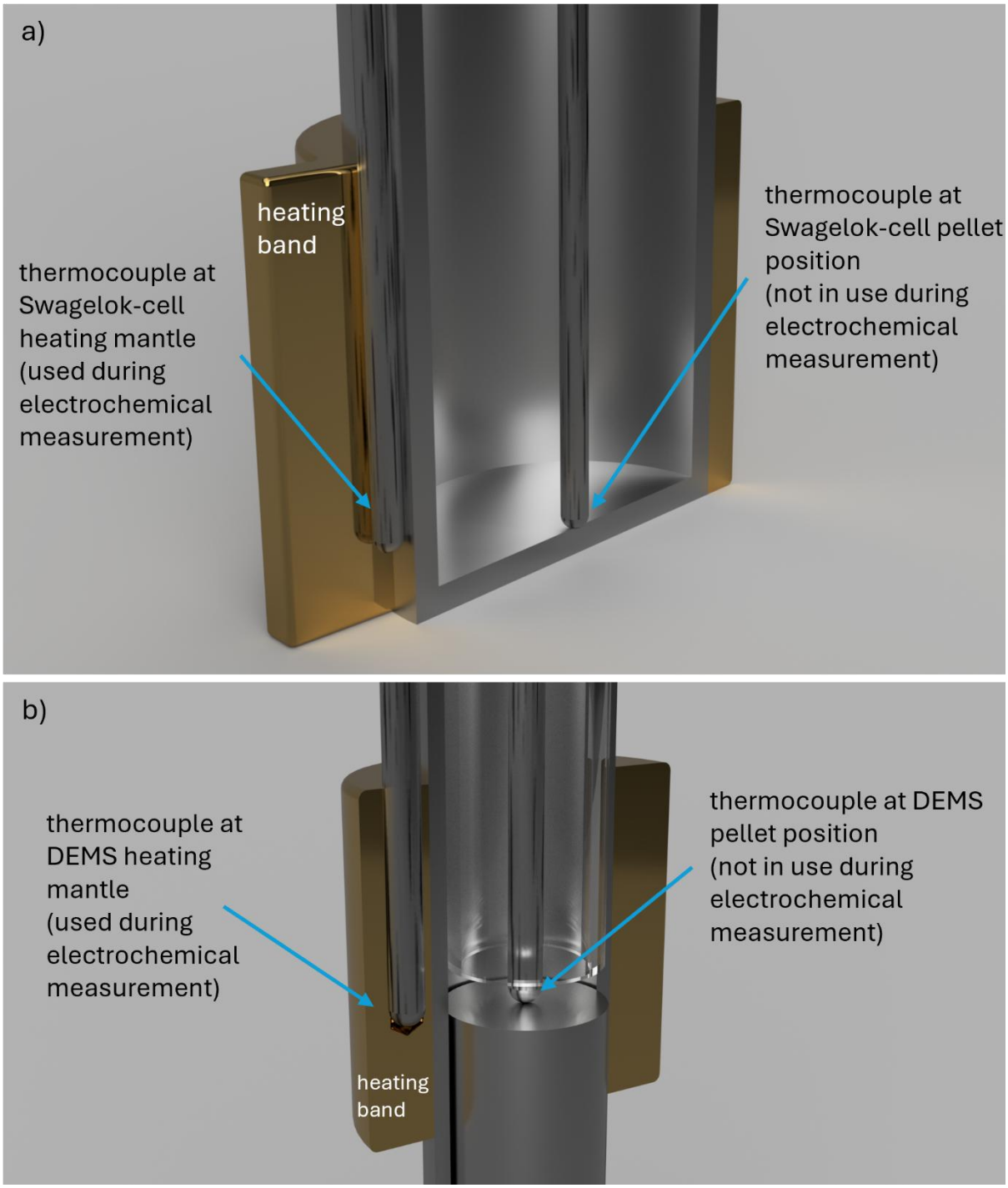

Figure S 5: Illustration of the test conducted to compare the temperature in (a) the typical Swagelok-cell configuration to (b) the temperature in the DEMS setup. The thermocouple at the pellet position in the Swagelok-cell showed 163 °C when the thermocouple at the heating band showed 170 °C (temperature stated in previous publications). Therefore, the temperature of the thermocouple at the heating band in the DEMS setup had to be adjusted to 197 °C to achieve 163 °C at the thermocouple at the pellet position in the DEMS setup. The temperatures stated in the main manuscript refer to the temperature at the pellet position.

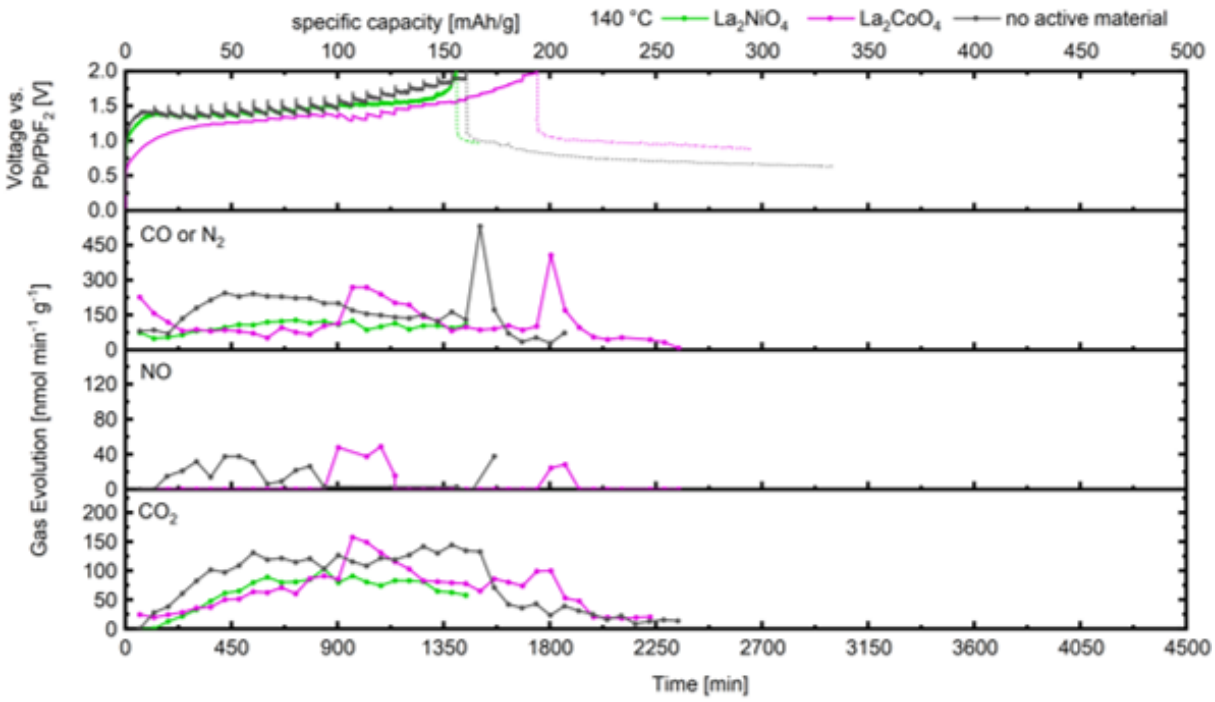

Figure S 6: DEMS measurement of La_2CoO_4, La_2NiO_4 and a composite without active material in electrochemical fluorination at 140 °C. Dotted lines in the potential graph indicate that the charging has stopped and the cell is now in relaxation. The mass spectrometer was calibrated for CO_2 by measuring air (420 ppm of CO_2). The values for CO/N_2 and NO are to be considered semi-quantitative. The capacity for the cell without active material is calculated for the same mass of active material used in the cells containing either La_2CoO_4 or La_2NiO_4. Since the mass of carbon is the same in all these cells, this way of depicting the capacity best reflects the contribution of carbon to the capacity and gas evolution for the cells containing active materials.

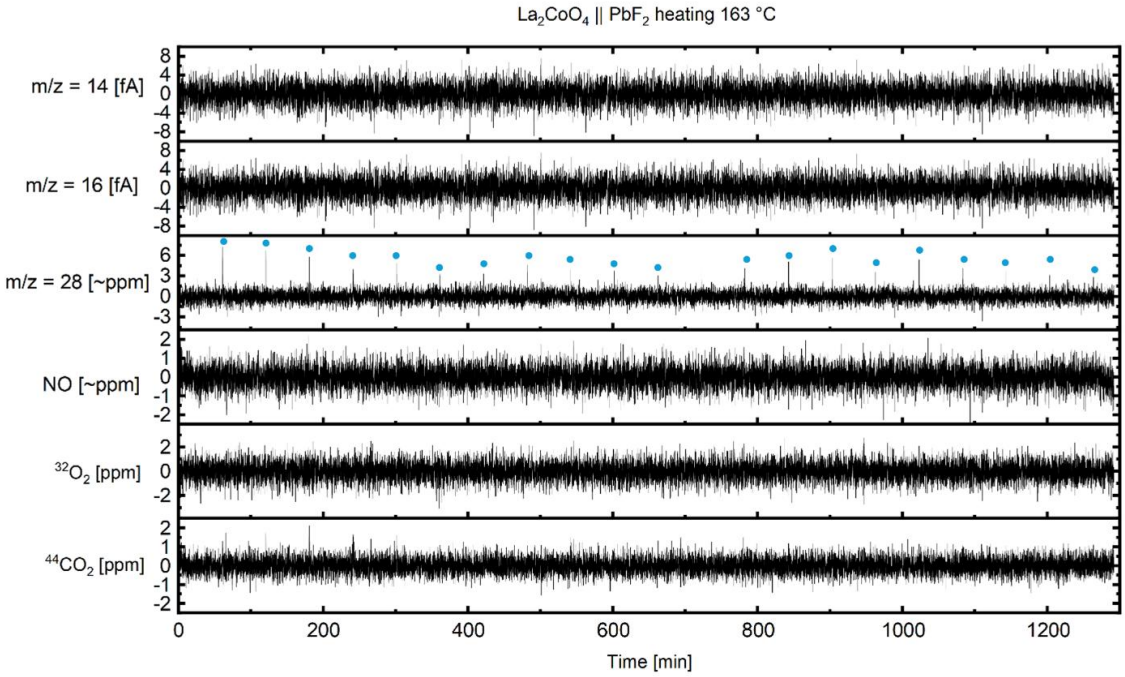

Figure S 7: Gas evolution measurement of a La_2CoO_4 || PbF_2 cell which has been heated at 163 °C without applied electrochemistry. Blue dots mark the peaks in the signal for m/z = 28 in regular 1 h intervals which mark outgassing of adsorbed nitrogen.

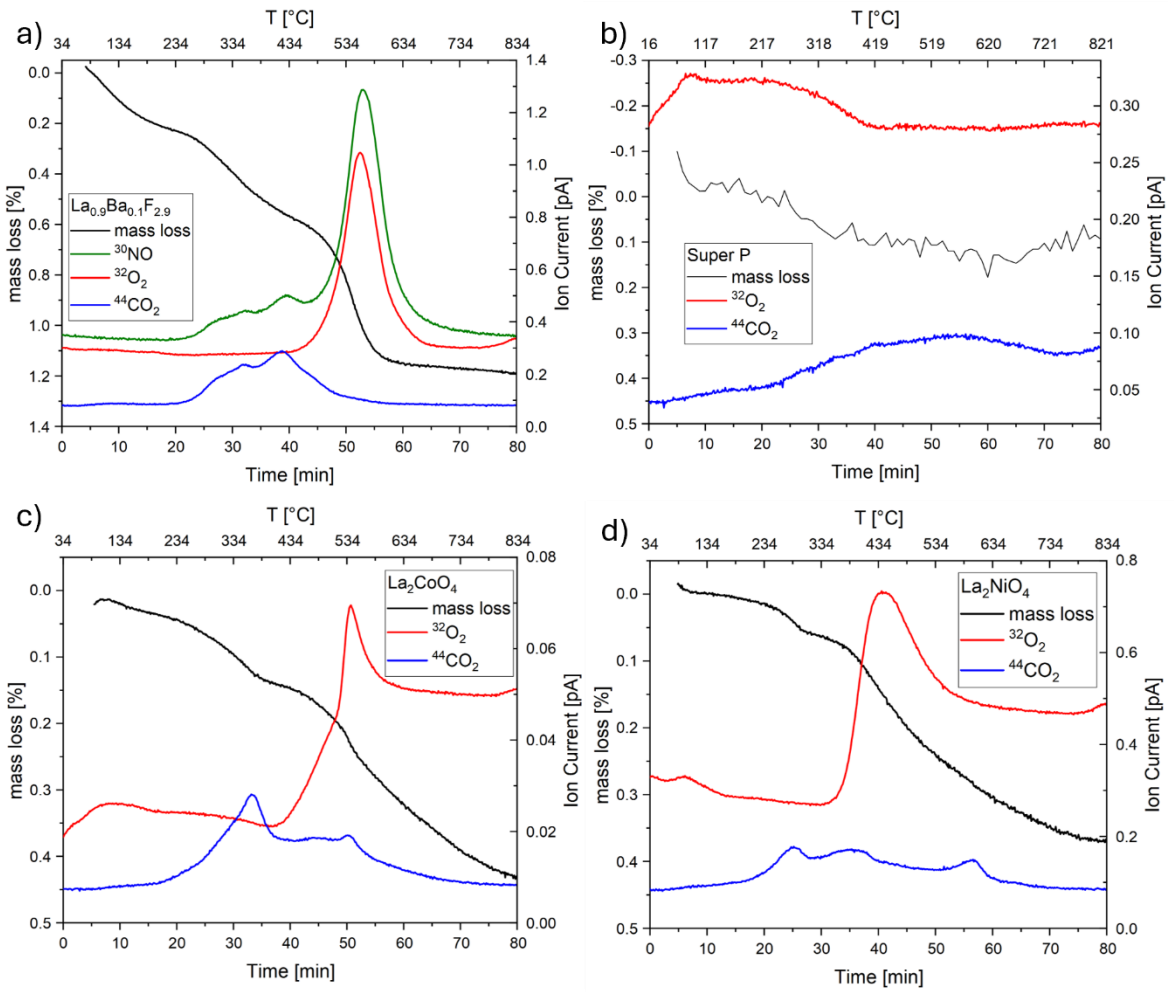

Figure S 8: TG-MS data of the precursor materials used for the cathode composites tested in the DEMS measurements (a) $La_{0.9}Ba_{0.1}F_{2.9}$ (b) Super P (c) La_2CoO_4 and (d) La_2NiO_4.

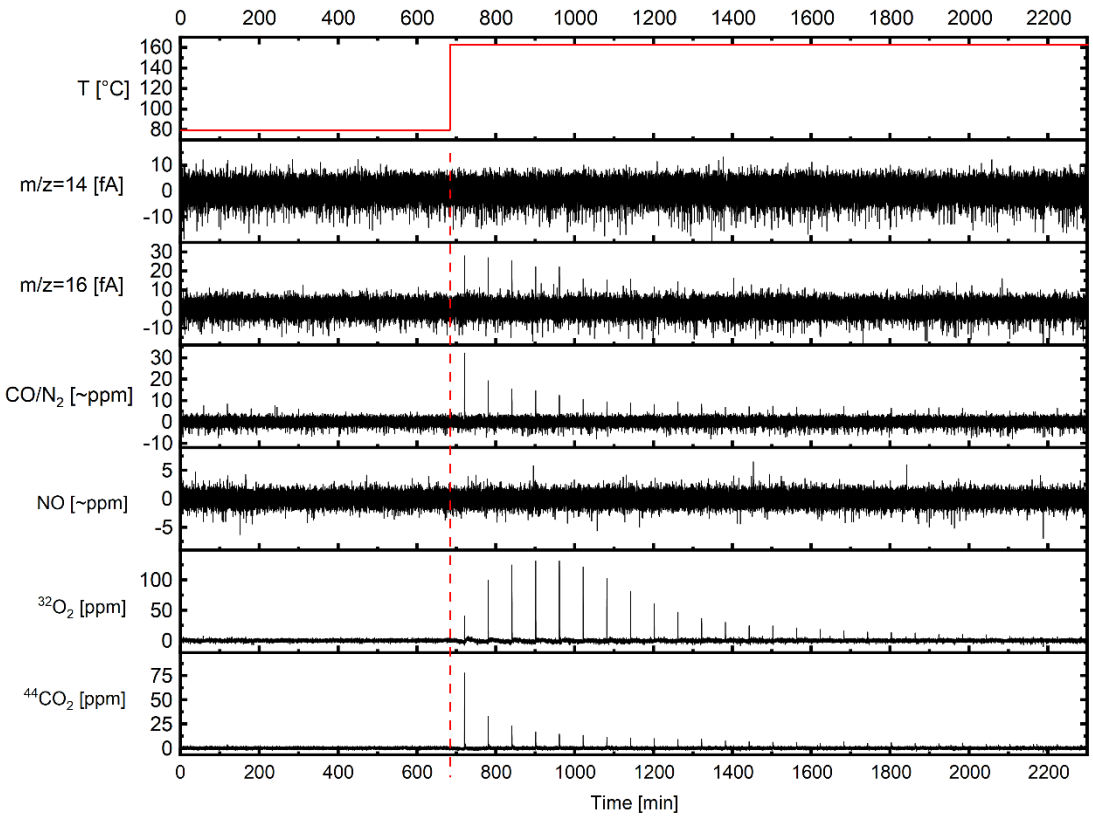

Figure S 9: Monitoring of the thermal decomposition of $KMnO_4$ in the presence of La_2CoO_4 in the DEMS setup. The temperature was held at 80 °C for 12 h to completely outgas adsorbed nitrogen, then increased to 163 °C to start the decomposition of $KMnO_4$. Note that while secondary reactions of evolved oxygen lead to the formation of CO and CO_2, a signal for molecular oxygen is always visible additionally.

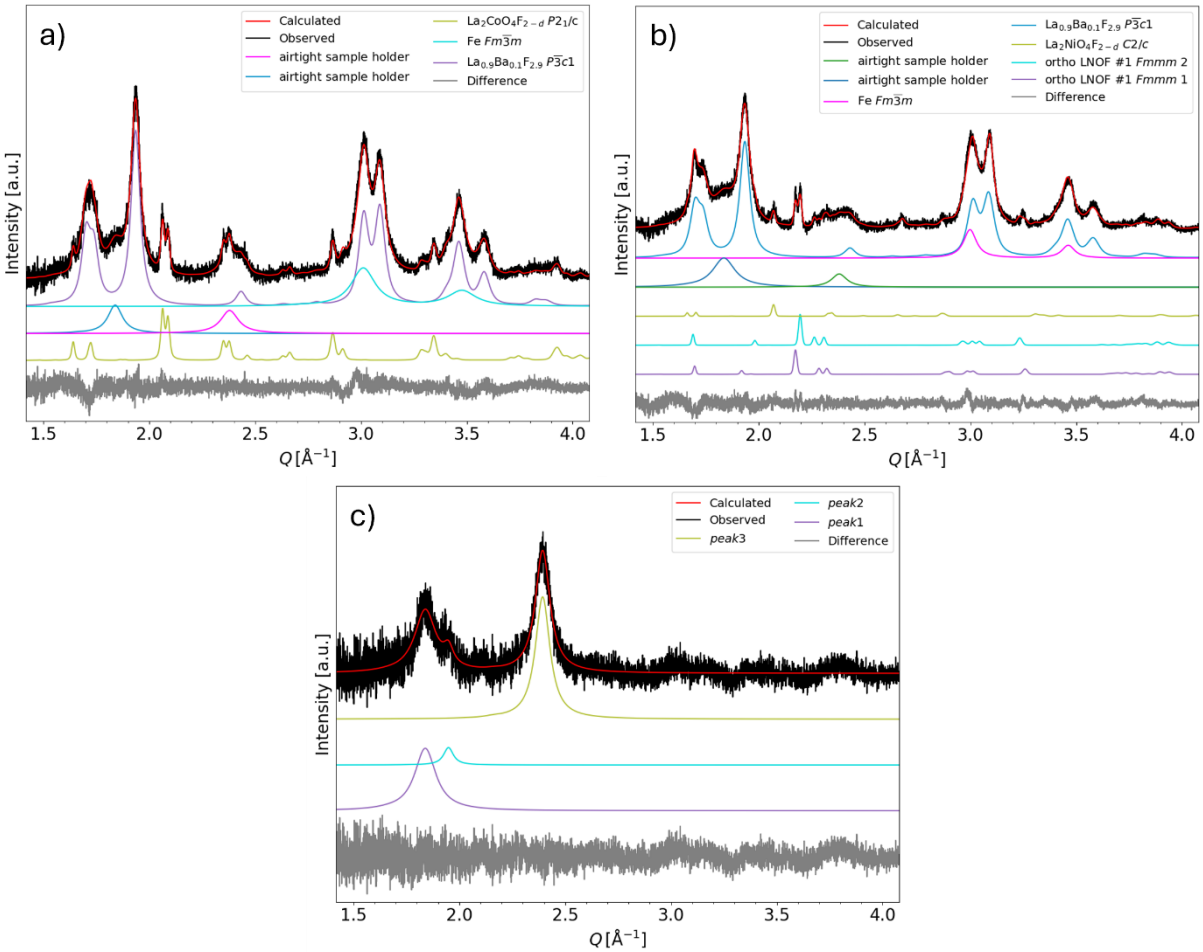

Figure S 10: XRDs of (a) La_2CoO_4- and (b) La_2NiO_4-based cathode composites after fluorination in the DEMS setup at 140 °C and. An unknown reflection appears around q ~ 2.9 $Å^{-1}$ for both in different extent, which is most likely a reflection of the stainless-steel airtight sample holder which appears in varying extent due to beam-overspill. Due to the strong microstructural broadening of the reflections, the $K_{\alpha 2}$ reflection cannot be recognized in these patterns. A background was subtracted from the patterns shown in this figure. Two reflections originating from the airtight sample holder can be found at q ~ 1.8 $Å^{-1}$ and q ~ 2.4 $Å^{-1}$ (c)

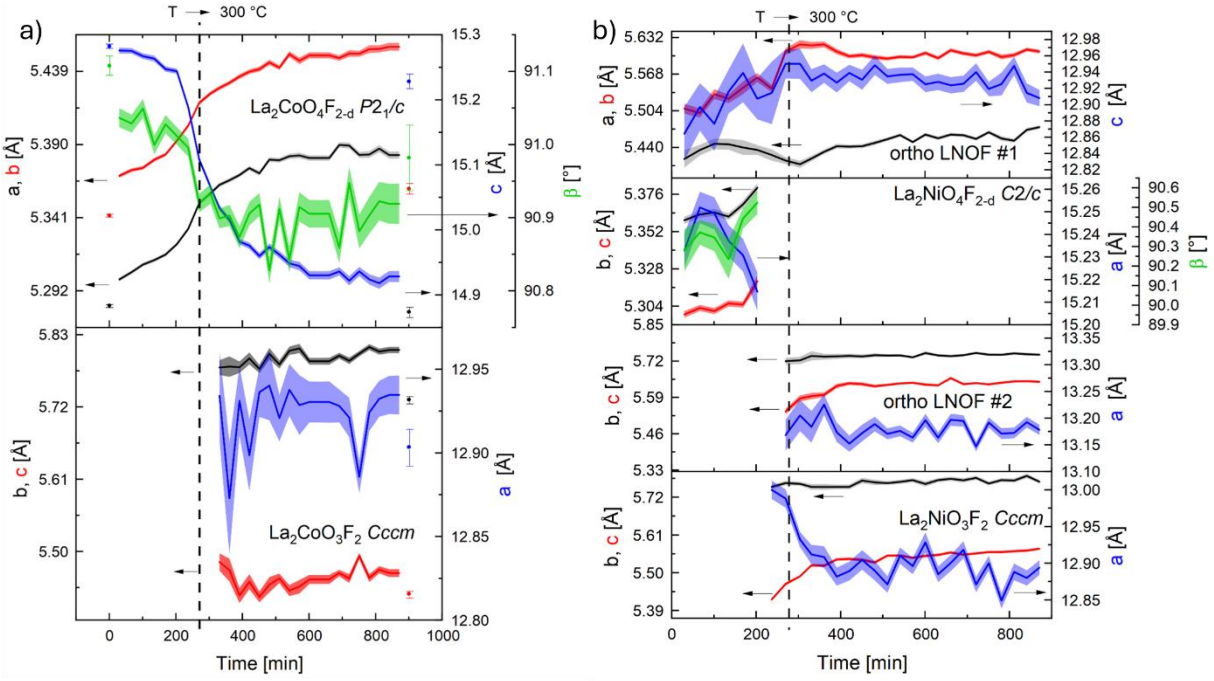

Figure S 11: Lattice parameters of all RP-phases obtained by Rietveld-refinement of the variable-temperature XRD patterns of the electrochemically fluorinated (a) La_2CoO_4 and (b) La_2NiO_4 pellet shown in Figure 6a and b respectively. The dashed line marks the time when 300 °C was reached. Values are only shown if the weight fraction is larger than 3 wt. %.

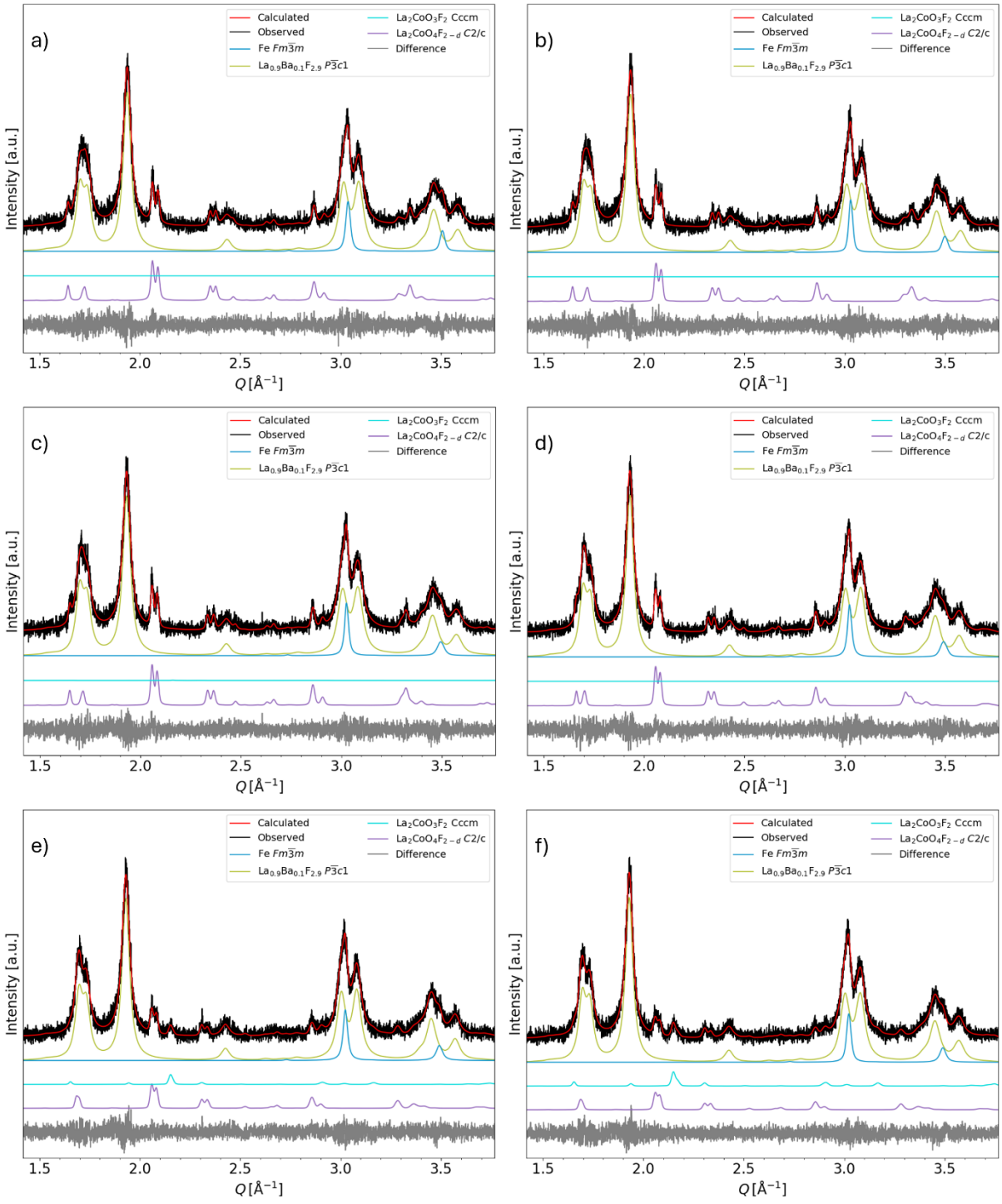

Figure S 12: plots of selected scans of the VTXRD measurement of the charged La_2CoO_4 cathode composite at (a) 25 °C (b) 160 °C (c) 240 °C (d) 0 minutes at 300 °C (e) 300 minutes at 300 °C and (f) 600 minutes at 300 °C. The steel sample stage used in the VTXRD measurement also produces a peak at q ~ 3.1 Å^{-1}. Due to the strong microstructural broadening of the reflections, the $K_{\alpha 2}$ reflection cannot be recognized in these patterns. A background was subtracted from the patterns shown in this figure. The peak position is different due to different measurement geometry, affecting the displacement of the steel and a different alloy being used.

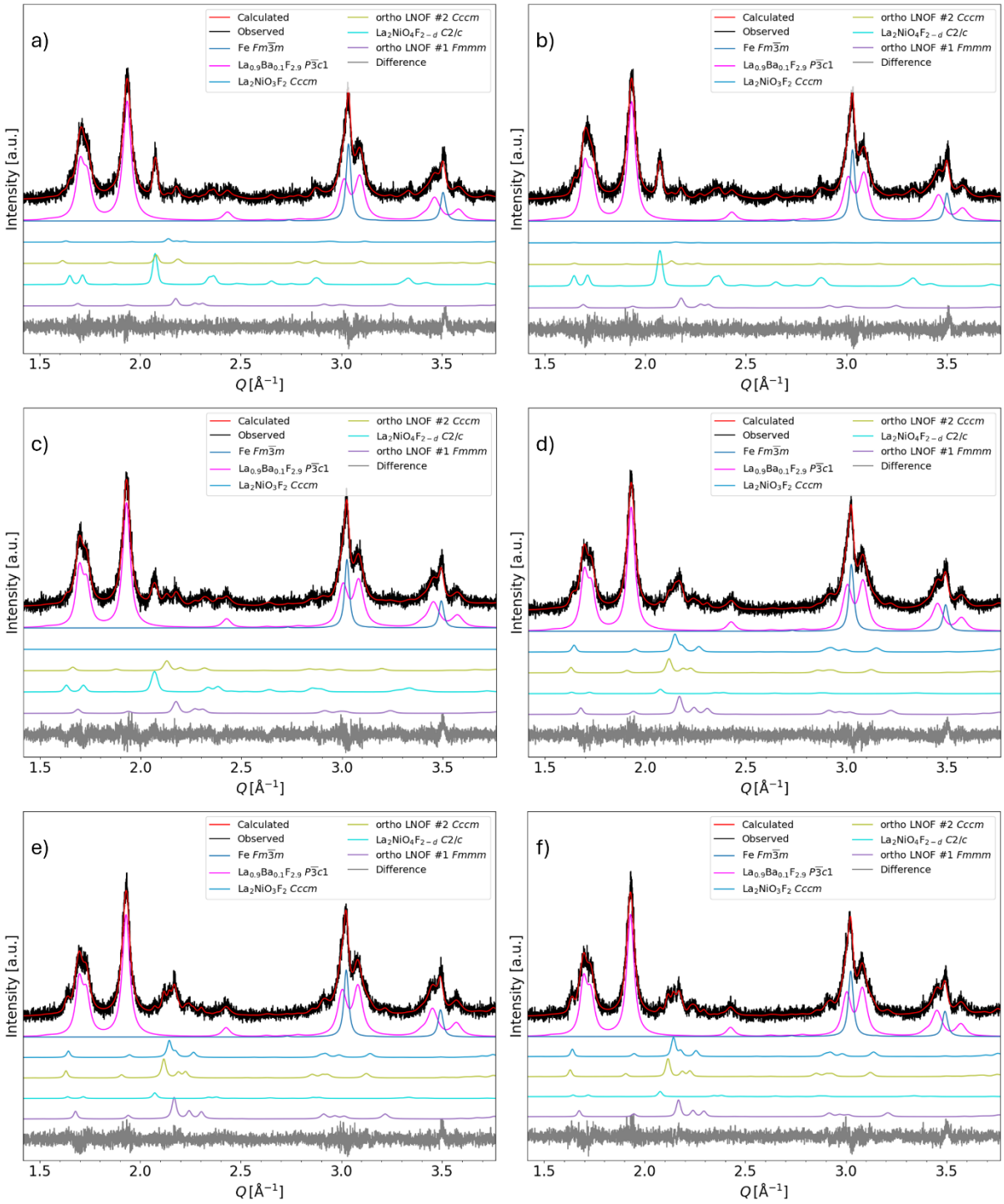

Figure S 13: plots of selected scans of the VTXRD measurement of the charged La_2NiO_4 cathode composite at (a) 25 °C (b) 160 °C (c) 280 °C (d) 150 minutes at 300 °C (e) 300 minutes at 300 °C and (f) 600 minutes at 300 °C. The steel sample stage used in the VTXRD measurement also produces a peak at q ~ 3.1 Å^{-1}. Due to the strong microstructural broadening of the reflections, the $K_{\alpha 2}$ reflection cannot be recognized in these patterns. A background was subtracted from the patterns shown in this figure. The peak position is different due to different measurement geometry, affecting the displacement of the steel and a different alloy being used.